Novel Magnetic and Optical Properties of $Sn_{1-x}Zn_xO_2$ Nanoparticles

Nevil A. Franco: McNair Scholar

Dr. Alex Punnoose: Mentor

Physics

Abstract

In this work, we report on the effects of doping SnO_2 nanoparticles with Zn^{2+} ions. A series of ~2- 3nm sized $Sn_{1-x}Zn_xO_2$ crystallite samples with $0 \leq x \leq 0.18$ were synthesized using a forced hydrolysis method. Increasing dopant concentration caused systematic changes in the crystallite size, oxidation state of Sn, visible emission and band gap of SnO_2 nanoparticles. X-ray Diffraction (XRD) studies confirmed the SnO_2 phase purity and the absence of any impurity phases. Magnetic measurements at room temperature showed a weak ferromagnetic behavior characterized by an open hysteresis loop. Their saturation magnetization M_s increases initially with increasing Zn concentrations, however for $x > 0.06$, M_s decreases. Samples with the highest M_s values ($x = 0.06$) were analyzed using an Inductively Coupled Plasma Mass Spectrometer (ICP-MS), looking for traces of any magnetic elements in the samples. Concentrations of all transition metals (Fe, Co, Mn, Cr, Ni) in these samples were below ppb level, suggesting the observed magnetism is not due to random inclusions of any spurious magnetic impurities and it cannot be explained by the existing models of magnetic exchange. A new visible emission near 490nm appeared in the Zn doped SnO_2 samples in the photoluminescence (PL) spectra which strengthened as x increased, suggesting the formation of defects such as oxygen vacancies. X-ray Photoelectron Spectroscopy (XPS) confirmed the nominal Zn dopant concentrations and the 2+ oxidation state of Zn in the $Sn_{1-x}Zn_xO_2$ samples. Interestingly, the XPS data indicated the presence of a small fraction of Sn^{2+} ions in $Sn_{1-x}Zn_xO_2$ samples in addition to the expected Sn^{4+}, and the Sn^{2+} concentration increased with increasing x. The presence of multi-valent metal ions and oxygen defects in high surface area oxide nanoparticles have been proposed as a potential recipe for weak ferromagnetism[1].

Introduction

SnO_2 is an interesting metal oxide that has been extensively studied for its magnetic, optical, and electrical properties[2,3]. It has been reported that some of these intrinsic properties have been induced by doping with transition metals[4,5] (e.g., Fe, Co, Mn, etc.). The one tailored physical property that falls into controversy is the induced magnetism that arises when doped with magnetic ions. The origin of room-temperature ferromagnetism (RTFM) has been debated to arise from either unintentional impurity inclusion, clusters[6] formed by the doped transition metals or defects in the metal oxides[7] such as oxygen vacancies. There have also been reports that RTFM has been observed in metal oxides that are either undoped[8,9] or doped with non-magnetic elements[10]. In this work, we make multiple sets of $Sn_{1-x}Zn_xO_2$ (with x increasing systematically from x = 0 to 0.18,) samples to confirm the reproducibility and repeatability of the novel properties induced by doping SnO_2 nanoparticles with Zn.

Experimental Methods & Results

$Sn_{1-x}Zn_xO_2$ nanoparticles were made in a powered form by reacting appropriate amounts of high quality tin (IV) acetate, anhydrous zinc acetate, urea, and nano-pure H_2O. The measured out precursors were put into a 250 mL round-bottom flask with a stir bar. The flask was set in a silicon oil bath for an hour and a half, while stirring. Bringing the flask down to room temperature, appropriate amounts of the solution were put into centrifuge tubes and spun at 10 to 20krpm, subsequently washed with nano pure H_2O and ethanol in between. The dopant concentrations employed were calculated using a molar ratio ([Zn]/[Zn]+[Sn]).

XRD patterns (Fig. 1) showed the single-phase cassiterite structure of SnO_2 with no secondary phases up to x = 0.18. The lattice parameters and average crystallite sizes were determined by Rietveld refinement methods[11]. It showed that as x increases, the crystallite size steadily reduced from 3.2 ± 0.3 nm to 2.2 ± 0.2nm, in agreement with

similar results observed by other groups also[12]. There seems to be a nucleation that occurs on the surface due to the introduction of zinc, causing interstitial defects which leads to the formation of tiny crystals[13]. The lattice parameters obtained by these refinement methods[11,14] also showed weak changes with the lattice volume increasing from 72.44 $Å^3$ to 72.58 $Å^3$ as Zn doping increased from 1% to 18%. Such weak changes in the lattice parameters is not unexpected when Zn^{2+} ions (0.72 Å) take on the tetrahedral sites of Sn^{4+} (0.69 Å) along with formation of additional oxygen vacancies necessary for charge compensation.

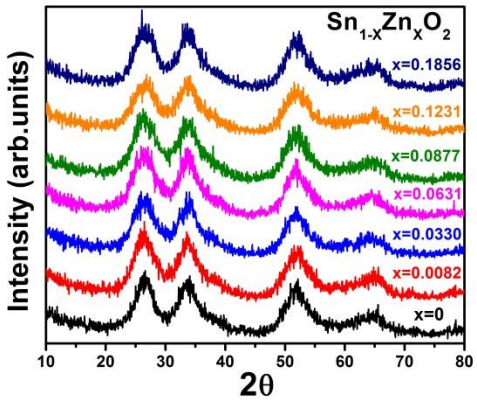

Figure 1. XRD patterns of $Sn_{1-x}Zn_xO_2$ samples with different Zn dopant concentration x, as indicated. The characteristic peaks broaden as x increases suggesting that crystallite size reduces.

Magnetic measurements were carried out at room temperature with a Vibrating Sample Magnetometer. A weak room-temperature ferromagnetic (RTFM) signal appears in the samples at low values of x, which increases and reaches a maximum saturation magnetization M_s ~1.5 memu/g for x = 0.06, as shown here in Fig. 2. This shows that the induced magnetism is directly dependent on the increasing introduction of zinc into the structure. Great care and consideration was taken when making these samples as to avoid any type of contamination. Since it is common to speculate that presence of magnetic impurities and/or transition metal ions act as the source of magnetism in these otherwise non-magnetic materials like SnO_2, several samples that showed relatively high M_s values were ran through an ICP-MS and the data ruled out any such impurity contributions since the measured concentrations of transition metals in these samples were well below parts per billion level (see Table 1). It may be noted that there have been reports of ferromagnetic behavior in $Sn_{1-x}Zn_xO_2$ based on both experimental[15] and computational[16,17] studies.

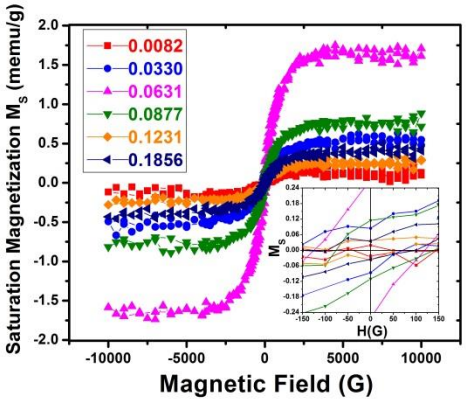

Figure 2. Hysteresis loops of $Sn_{1-x}Zn_xO_2$ nanoparticles displaying characteristic ferromagnetic behavior. Inset shows the low-field range to highlight the open hysteresis loops and coercivity.

Table 1. Concentrations of selected transition metals measured using ICP-MS from three independent sets of $Sn_{0.94}Zn_{0.06}O_2$ samples, confirming that any magnetic impurity presence is below ppb levels.

Transition Metals Tested	Chromium	Manganese	Iron	Cobalt	Nickle	Zinc
Units (Parts per billion)	ppb	ppb	ppb	ppb	ppb	ppb
First Set	0.254	0.138	0.835	0.256	0.799	1327
Second Set	0.007	0	0	0.234	0.619	1277
Third Set	0.166	0.047	0	0.264	0.355	1538

The PL and band gap energy of the samples were measured at 10 K using a 325 nm line of a He-Cd laser for excitation and the spectra are shown in Fig. 3. Sharp peaks observed at ~3.75 eV are due to Raman scattering due to the band gap approaching the excitation laser line[14]. Bulk SnO_2 has a band gap of 3.6 eV, but it is not photoluminescent. When impurities like Zn^{2+} ions are incorporated into the structure of SnO_2 nanocrystals, the resulting structural and chemical changes might modify non-radiative centers to become active. High density of oxygen vacancies formed by the introduction of Zn leads to interaction with interfacial Sn that might lead to the formation of a considerable amount of trapped states within the band gap of SnO_2, giving rise to high PL mixed peaks (~3.35 eV) observed in the samples with $x \geq 0.12$. In a similar experiment[13] with Zn doped SnO_2 nanoparticles, room-temperature PL measurements have shown similar peaks, shifted to lower energies. As x increases, another important change observed is the emergence and gradual strengthening of the green band (~2.5 eV), which is commonly attributed to oxygen vacancies, most likely occurring on the surface of the nanocrystals. In samples with x = 0.18, we see a slight blue shift of this green band. This green band has appeared in related works[18,19] that studied the optical properties of SnO_2 strictly relating it to oxygen vacancies. It is likely that the changes seen in both the UV and green emissions may be related to the extensive structural and chemical changes effected by the increasing Zn incorporation and the ferromagnetic signal induced in the samples also may be related to these chemical and structural changes.

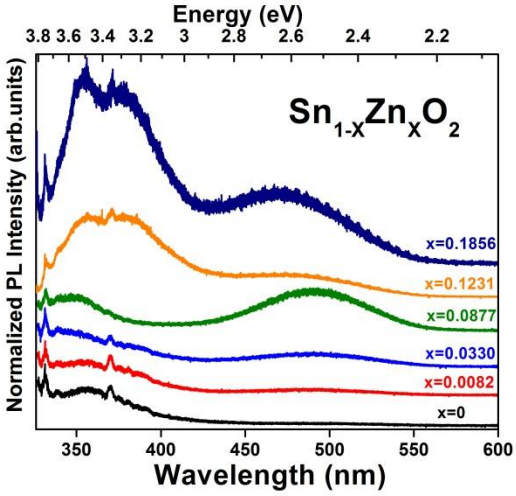

Figure 3. PL spectra of $Sn_{1-x}Zn_xO_2$ samples, showing both the UV band edge transition and the green emission. The sharp peaks just below 350 nm are due to Raman scattering.

The chemical states of tin and zinc ions and their binding energies (BE) are shown in the high resolution XPS spectra (Fig. 4). The BE of Zn $2p_{3/2}$ peak is around 1021.3 eV; the slight change in the BE to that of bulk ZnO (1021.8 eV) may be due to the presence of additional defects in these nanoscale samples. The Zn $2p_{3/2}$ peak becomes more intense as x goes up, giving evidence for the increasing incorporation of Zn^{2+} into the crystal structure of SnO_2. The Sn^{4+} $3d_{5/2}$ and $3d_{3/2}$ states at BE ~486 eV and ~495 eV respectively, have a separation of 9.3 eV as seen in SnO_2[20] and are present in all samples. However, in samples with higher x values, an Sn^{2+} shoulder begins to

emerge and gradually intensifies, showing that in the $Sn_{1-x}Zn_xO_2$ nanocrystals, Zn^{2+} ions are creating new defects such as Sn^{2+}, most likely on their surface region. With this mix of states, it is difficult to distinguish the BE of the Sn 3*d* states although it has been reported[21] that the BE of Sn^{2+} (~485.9 eV) is a little lower than the BE of Sn^{4+} (~486.6 eV). This supports the increasing formation of Sn^{2+} states in the high Zn doped SnO_2 samples.

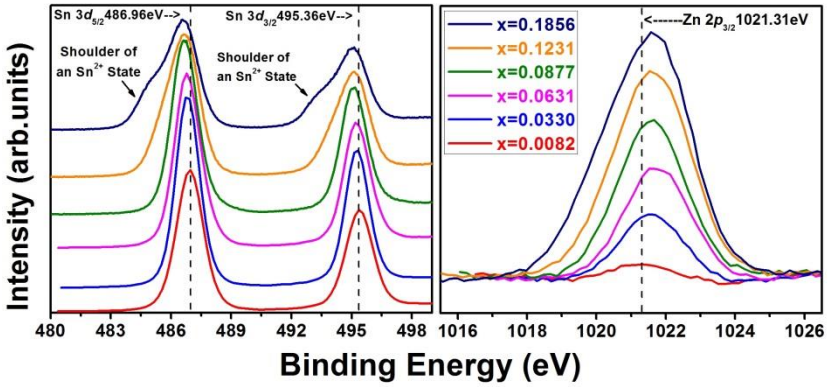

Figure 4. High resolution XPS spectra of $Sn_{1-x}Zn_xO_2$ nanocrystals, highlighting the Sn 3*d* and Zn 2*p* regions.

Conclusion

In conclusion, we have synthesized and investigated these powdered nanocrystalline samples of SnO_2 successfully doped with zinc ($0 \leq x \leq 0.18$). Zn doping causes significant changes in the SnO_2 crystal structure and oxidation state of Sn, and it introduces large number of defects. The incorporation of Zn produces many new properties in SnO_2, including weak RTFM characterized by open hysteresis loops, and new and enhanced luminescent emissions. Zn^{2+} doping seems to introduce new Sn^{2+} states and presumably more oxygen vacancies, which are likely at work in the observed new magnetic and optical properties. Lack of any measureable concentration of magnetic ions in these $Sn_{1-x}Zn_xO_2$ nanocrystals makes it difficult to justify the observed RTFM by any of the known exchange mechanisms. The emergence of these observed properties may be related to changes in the electronic structure of SnO_2 due to the incorporation of Zn dopants, defects and the nanoscale size of the particles. The XPS spectrum indicates the existence of Sn in both Sn^{2+} and Sn^{4+} states in our samples. Doping Sn^{4+} states with Zn^{2+} ions and conversion of some Sn^{4+} ions into Sn^{2+} states are likely to introduce defect states such as oxygen vacancies. However, more detailed studies are necessary to confirm these possibilities and this will be pursued in future studies.

Acknowledgements

The authors would like to thank support by NSF CBET 1134468, NSF EAGER DMR-1137419, and ARO W911NF-09-1-0051 grants. Help from Dr. Marion Lytle and Daniel Hillsberry is acknowledged.

References

[1] J. M. D. Coey, P. Stamenov, R. D. Gunning, M. Venkatesan, and K. Paul, New Journal of Physics **12** (2010).

[2] P. Chetri and A. Choudhury, Physica E-Low-Dimensional Systems & Nanostructures **47**, 257 (2013).

[3] C. T. Wang, D. L. Lai, and M. T. Chen, Applied Surface Science **257** (1), 127 (2010).

[4] G. A. Alanko, A. Thurber, C. B. Hanna, and A. Punnoose, Journal of Applied Physics **111** (7) (2012).

[5] Z. M. Tian, S. L. Yuan, J. H. He, P. Li, S. Q. Zhang, C. H. Wang, Y. Q. Wang, S. Y. Yin, and L. Liu, Journal of Alloys and Compounds **466** (1-2), 26 (2008).

[6] I. M. L. Billas, A. Chatelain, and W. A. Deheer, Science **265** (5179), 1682 (1994).

[7] N. H. Hong, J. Sakai, N. T. Huong, N. Poirot, and A. Ruyter, Physical Review B **72** (4) (2005).

[8] J. M. D. Coey, M. Venkatesan, P. Stamenov, C. B. Fitzgerald, and L. S. Dorneles, Physical Review B **72** (2) (2005).

[9] L. Zhang, S. H. Ge, and Y. L. Zuo, Journal of the Electrochemical Society **157** (8), K162 (2010).

[10] H. Saeki, H. Tabata, and T. Kawai, Solid State Communications **120** (11), 439 (2001).

[11] L. Lutterotti, S. Matthines, and H.R. Wenk, in *12th Annual International Conference on Textures of Materials* (NCR Press, Ottawa, Canada, 1999), Vol. 1, p. 1599.

[12] Z. R. Li, X. L. Li, X. X. Zhang, and Y. T. Qian, Journal of Crystal Growth **291** (1), 258 (2006).

[13] P. P. Sahay, R. K. Mishra, S. N. Pandey, S. Jha, and M. Shamsuddin, Current Applied Physics **13** (3), 479 (2013).

[14] Katie Rainey, Jordan Chess, Josh Eixenberger, D. Tenne, Charles Hanna, and Alex Punnoose, Journal of Applied Physics **115**, 17D727 (2013).

[15] Xiaofang Liu, Javed Iqbal, Zhangben Wu, Bo He, and Ronghai Yu, Journal of Physical Chemistry C **114** (11), 4790 (2010).

[16] W. Wei, Y. Dai, M. Guo, K. R. Lai, and B. B. Huang, Journal of Applied Physics **108** (9) (2010).

[17] Y. L. Zhang, X. M. Tao, and M. Q. Tan, Journal of Magnetism and Magnetic Materials **325**, 7 (2013).

[18] S. H. Luo, P. K. Chu, W. L. Liu, M. Zhang, and C. L. Lin, Applied Physics Letters **88** (18) (2006).

[19] Ping Wu, Qiang Li, Xianquan Zou, Wende Cheng, Danli Zhang, Chuanxi Zhao, Lingfei Chi, and Tan Xiao, Journal of Physics: Conference Series (online) **188** (1), 8 (2009).

[20] Q. H. Wu, J. Song, J. Y. Kang, Q. F. Dong, S. T. Wu, and S. G. Sun, Materials Letters **61** (17), 3679 (2007).

[21] M. Kwoka, L. Ottaviano, M. Passacantando, S. Santucci, G. Czempik, and J. Szuber, Thin Solid Films **490** (1), 36 (2005).